

Transformer Meets Gated Residual Networks To Enhance Photoplethysmogram Artifact Detection Informed by Mutual Information Neural Estimation

Thanh-Dung Le, *Member, IEEE*, Philippe Jovet, and Rita Noumeir, *Member, IEEE*

Abstract—This study delves into the effectiveness of various learning methods in improving Transformer models, focusing particularly on the Gated Residual Network Transformer (GRN-Transformer) in the context of pediatric intensive care units (PICU) with limited data availability. Our findings indicate that Transformers trained via supervised learning are less effective compared to MLP, CNN, and LSTM networks in such environments. Yet, leveraging unsupervised and self-supervised learning on unannotated data, with subsequent fine-tuning on annotated data, notably enhances Transformer performance, although not to the level of the GRN-Transformer. Central to our research is the analysis of different activation functions for the Gated Linear Unit (GLU), a crucial element of the GRN structure. We also employ Mutual Information Neural Estimation (MINE) to evaluate the GRN's contribution. Additionally, the study examines the effects of integrating GRN within the Transformer's Attention mechanism versus using it as a separate intermediary layer. Our results highlight that GLU with sigmoid activation stands out, achieving 0.98 accuracy, 0.91 precision, 0.96 recall, and 0.94 F1 score. The MINE analysis supports the hypothesis that GRN enhances the mutual information between the hidden representations and the output. Moreover, the use of GRN as an intermediate filter layer proves more beneficial than incorporating it within the Attention mechanism. In summary, this research clarifies how GRN bolsters GRN-Transformer's performance, surpassing other learning techniques. These findings offer a promising avenue for adopting sophisticated models like Transformers in data-constrained environments, such as PPG artifact detection in PICU settings.

Index Terms—clinical PPG signals, Transformers, Gated Residual Networks, imbalanced classes, and artifact detection.

I. INTRODUCTION

Recently, the Pediatric Intensive Care Unit (PICU) at CHU Sainte-Justine (CHUSJ) has achieved significant progress by establishing a high-resolution research database (HRDB) [1], [2]. This state-of-the-art database seamlessly integrates biomedical signals from various monitoring devices into the electronic patient record, enhancing data continuity throughout a patient's PICU stay [3]. The implementation of HRDB

This work was supported in part by the Natural Sciences and Engineering Research Council (NSERC), in part by the Institut de Valorisation des données de l'Université de Montréal (IVADO), in part by the Fonds de la recherche en sante du Quebec (FRQS).

Thanh-Dung Le is with the Biomedical Information Processing Lab, École de Technologie Supérieure, University of Québec, Montréal, Québec, Canada (Email: thanh-dung.le.1@ens.etsmtl.ca).

Philippe Jovet is with the CHU Sainte-Justine Research Center, CHU Sainte-Justine Hospital, University of Montreal, Montréal, Québec, Canada.

Rita Noumeir is with the Biomedical Information Processing Lab, École de Technologie Supérieure, University of Québec, Montréal, Québec, Canada.

has notably improved the Clinical Decision Support System (CDSS) at CHUSJ, elevating patient safety and supporting decision-making with substantial evidence [4]. A critical aim of the CDSS at CHUSJ is the prompt and precise diagnosis of acute respiratory distress syndrome (ARDS). Monitoring Oxygen saturation (SpO₂) values, crucial for ARDS diagnosis, is key in predicting and managing ARDS [5], [6]. These values are also vital in determining respiratory support strategies [7]–[9]. Additionally, the ability to predict SpO₂ from Photoplethysmography (PPG) waveforms and non-invasive blood pressure estimation is increasingly acknowledged as crucial for enhancing CDSS functionalities [10], [11]. Therefore, accurately identifying and discarding erroneous waveforms and SpO₂ values from CDSS inputs is of utmost importance. Maintaining the accuracy of these inputs is crucial for the effective operation of the CDSS, thereby directly influencing patient outcomes and the efficiency of care.

In this evolving landscape of clinical data utilization, our research turns to Photoplethysmography (PPG) artifact detection, leveraging machine learning (ML) techniques to enhance diagnostic accuracy. Previous studies, such as those by Macabiau et al. [12], have explored ML in this domain, yet challenges persist, particularly in scenarios with limited data and imbalanced classes. Traditional Transformer models, despite their advanced attention mechanisms, have shown limited effectiveness in these settings compared to other methods like semi-supervised label propagation and supervised KNN learning.

Our recent work has introduced a novel solution to these challenges: the integration of the Gated Residual Network (GRN) into the Transformer framework, creating the GRN-Transformer hybrid model [13]. This model outperforms traditional Transformer models in smaller datasets and other existing models in artifact detection accuracy and reliability. However, the reliance on annotated data remains a significant constraint in fully supervised ML algorithms, as highlighted in recent studies [14].

Addressing this constraint, we have explored the potential of self-supervised learning (SSL) to enhance Transformer performance. While SSL has improved the Transformer model, its performance still lags behind the GRN-Transformer. The Table I presents a comparative analysis of various Transformer-based models, including supervised, unsupervised, and self-supervised approaches, as well as the GRN-Transformer, in PPG artifact detection at CHUSJ. The GRN-Transformer emerges as the most proficient, particularly in accuracy and

TABLE I: A summary of Transformer’s performance for PPG artifact detection at CHUSJ

Transformer-based Models	Acc	Pre	Rec	F1
Supervised [12]	0.95	0.85	0.86	0.85
Unsupervised (AE) [14]	0.97	0.89	0.93	0.91
Self-supervised [14]	0.97	0.93	0.92	0.93
GRN-Transformer [13]	0.98	0.90	0.97	0.93

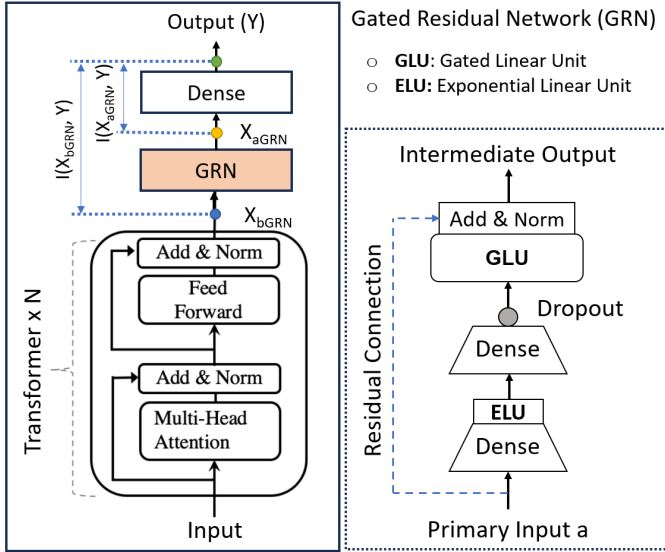


Fig. 1: An end-end process diagram workflow demonstration.

recall.

Building on these findings, our study aims to understand further and optimize the GRN-Transformer’s performance. We investigate the efficacy of different Gated Linear Unit (GLU) activation functions, the backbone of the GRN structure. Additionally, we employ Mutual Information Neural Estimation (MINE) [15] to evaluate the GRN’s contribution to the Transformer model. Our research also examines the effect of integrating GRN within the Transformer’s attention mechanism versus its traditional role as an external intermediate layer.

In summary, our study seeks to unravel the mechanisms behind the enhanced performance of GRN-Transformers over other learning methods. By delving into the nuances of GLU activation functions and the positioning of GRN within the Transformer architecture, we aim to provide insights that could revolutionize the use of advanced ML models in data-limited environments like PPG artifact detection in PICU settings.

II. RELATED WORKS

Training Transformer models with small datasets pose significant challenges. These models typically exhibit a generalization gap and tend toward sharp minima in such contexts [16]. Furthermore, their efficacy diminishes when dealing with imbalanced and small PPG signals [17].

To mitigate these issues, various strategies have been proposed. One approach involves altering the attention mechanism and employing data augmentation methods [18]. Alternatively,

integrating Convolutional Neural Networks (CNNs) with the Transformer’s attention mechanism has been explored [19]. However, these solutions are not without drawbacks:

- 1) **Computational Complexity [20]**: Transformers are inherently resource-intensive, with the self-attention mechanism’s computational demands scaling quadratically with input length. Adding CNNs can further increase these demands, particularly for lengthy data sequences, potentially making it unfeasible in certain scenarios.
- 2) **Sequential Processing in CNNs [21]**: CNNs process data in a sequential manner, focusing on small, localized regions. This approach hinders their ability to capture long-range dependencies effectively.

In addition to these methods, we introduce the Gated Residual Network (GRN) as a key component of a Transformer-based classifier. The GRN effectively handles uncertain input-target relationships, enabling nonlinear processing when necessary. A crucial feature of our GRN is the use of Gated Linear Units (GLUs) [22], which dynamically emphasize or suppress information based on task requirements. Such gating techniques have been utilized in various models, including Gated Transformer Networks [23] and Temporal Fusion Transformers [24]. According to [24], the GRN processes an input a , as illustrated in Fig. 1, with the following output:

$$\text{GRN}_\omega(a) = \text{LayerNorm}(a + \text{GLU}_\omega(\theta_1)), \quad (1)$$

$$\theta_1 = W_{1,\omega} \theta_2 + b_{1,\omega}, \quad (2)$$

$$\theta_2 = \text{ELU}(W_{2,\omega} a + b_{2,\omega}) \quad (3)$$

Here, θ_1 and θ_2 represent intermediate layers, LayerNorm denotes standard layer normalization, and ω indicates shared weights. The Exponential Linear Unit (ELU) activation function, defined as follows for $0 < \alpha$, is also employed:

$$f(x) = \begin{cases} x & \text{if } x > 0 \\ \alpha(\exp(x) - 1) & \text{if } x \leq 0 \end{cases} \quad (4)$$

Additionally, the GRN uses a GLU in its gating layers for architectural flexibility. Given input η , the GLU operates as follows:

$$\text{GLU}_\omega(\eta) = \sigma(W_{3,\omega}\eta + b_{3,\omega}) \odot (W_{4,\omega}\eta + b_{4,\omega}), \quad (5)$$

where $W_{(\cdot)}$ and $b_{(\cdot)}$ represent the weights and biases, respectively, \odot signifies the element-wise Hadamard product, and $\sigma(\cdot)$ denotes the sigmoid activation function:

$$\sigma(x) = \frac{1}{1 + \exp(-x)}. \quad (6)$$

The GLU enables the GRN to regulate the extent of its contribution to the input a . It can effectively bypass the layer by setting the GLU outputs near zero, thus suppressing nonlinear contributions. During training, dropout is applied before the gating layer and layer normalization, specifically to θ_1 in Eq. (2). This method enhances model robustness and helps prevent overfitting [25].

This study expands upon our previous research [17] by integrating a GRN as an intermediary layer within various classifiers, including the Transformer classifier, as depicted in Fig. 1. Termed the GRN-Transformer, this integration excels in handling small datasets and ambiguous input-target relationships. Its benefits are not limited to time-series data [23], [24] but extend to a wide range of data types [22], [25]. Incorporating GRN into the Transformer architecture marks a significant innovation of our work, greatly enhancing model performance and generalization across various domains.

III. MATERIALS AND METHODS

A. Clinical PPG Data at CHUSJ

The CHUSJ-PICU has developed a high-resolution research database (HRDB) that links biomedical signals from patient monitors to electronic patient records, capturing physiological data using both invasive and non-invasive methods. The database includes pulse oximetry for photoplethysmogram (PPG) signals and blood pressure measurements obtained through various techniques. This study, approved by the CHU Sainte Justine Hospital's ethics board (eNIMP:2023-4556), focuses on children aged 0 to 18 admitted between September 2018 and September 2023. It includes ECG, PPG, and arterial blood pressure (ABP) waveforms, excluding data after the fourth day of hospitalization and from patients on Extracorporeal Membrane Oxygenation (ECMO) or with multiple admissions. Ultimately, 1,573 patients were selected, with continuous 96-hour recordings of ECG, PPG, and blood pressure collected every 5 seconds at 128 Hz for PPG and 512 Hz for blood pressure and ECG. A 30-second window of PPG signals was specifically extracted for analysis.

In this study, data preprocessing comprises four key steps: filtering, segmentation, resampling and normalization, and feature extraction. Initially, signals undergo bandpass filtering through a Butterworth filter with 0.5 Hz to 5 Hz cut-off frequencies, using a forward-backward method to maintain signal integrity and remove noise. The segmentation process then divides the PPG signal into segments by identifying local minima, allowing for detailed artifact analysis within each pulse. Following this, each pulse is uniformly over-sampled to 256 samples to represent a 1-second heart cycle, with linear interpolation ensuring consistency across pulses. Normalization is applied to maintain uniform feature scaling. Finally, temporal features are extracted from each segment at four-millisecond intervals, resulting in 256 samples per pulse, effectively capturing the PPG signal's temporal behavior for further analysis and classification.

The study's data annotation process begins with a healthcare professional manually annotating PPG signal pulses to establish a reliable ground truth, crucial for evaluating classification algorithms and classifier performance. To augment this, an automated algorithm, acting as a pseudo-expert, reannotates 10% of the data initially reviewed by the human expert, using statistical techniques to ensure the pulses fall within expected parameters [17]. This dual-annotation approach enhances the accuracy and reliability of the motion artifact annotations. Furthermore, to optimize the ML algorithms for automatic

artifact classification. This approach, involving 1,571 signals with over 81,000 pulses and 256 features per pulse, helps identify the most efficient subset size for annotation.

B. Gated Linear Unit with Different Activation Functions

In the realm of neural networks, the choice of activation functions plays a pivotal role in determining the effectiveness and efficiency of learning algorithms. The Table presented summarizes various activation functions, each with its unique equation and characteristics, essential for different neural network applications. The classic Sigmoid function, known for its smooth gradient, is represented alongside its variant, the Hard Sigmoid, which offers a computationally simpler alternative. The Soft-Sign Sigmoid provides a balanced approach, while the Snake Periodic Function introduces a periodic component to the activation. The Linearly Scaled Hyperbolic Tangent (LiSHT) enhances the traditional tanh function with linear scaling. Widely used in deep learning, the Rectified Linear Unit (ReLU) and its variations like the Exponential Linear Unit (ELU), Gaussian Error Linear Unit (GELU), and Scaled Exponential Linear Unit (SELU) offer different approaches to handling negative input values. The Sigmoid-Weighted Linear Units (Swish) and Self Regularized Non-Monotonic Neural (Mish) functions further extend the repertoire of activation functions, providing flexibility and adaptability in neural network design and performance optimization [26], [27].

The table compares various Gated Linear Unit (GLU) models, each paired with a distinct activation function to create specialized GLU form functions. The BilinearGLU model employs a linear activation function, resulting in a straightforward GLU form. The standard GLU model uses the sigmoid function, while the hardGLU adapts the hard sigmoid (hard_σ) for its gating mechanism. The SoftsignGLU integrates the SoftSign activation, and the SnakeGLU incorporates the periodicity of the Snake function. LiGLU utilizes the Linearly Scaled Hyperbolic Tangent (LiSHT), adding a non-linear, scaled twist. The ReGLU, EGLU, GEGLU, and SeGLU models apply the ReLU, ELU, GELU, and SELU functions, respectively, each adding its unique characteristics to the gating process. SwiGLU and MiGLU explore the dynamics of Sigmoid-Weighted Linear Units (Swish_β) and the Self Regularized Non-Monotonic Neural (Mish) functions, respectively. Each model's GLU form function follows a similar pattern, combining the chosen activation function with linear transformations to modulate the input signal effectively.

C. Mutual Information Neural Estimation

"Mutual Information Neural Estimation" presents a new approach for estimating mutual information between high-dimensional continuous random variables using gradient descent over neural networks. The authors introduce the Mutual Information Neural Estimator (MINE), which is scalable in both dimensionality and sample size and can be trained via back-propagation. MINE is shown to be effective in various applications, including enhancing adversarially trained generative models and implementing the Information Bottleneck for

TABLE II: List of activation functions [26], [27]

Name	Equation
Sigmoid	$\frac{1}{1+e^{-x}}$
Hard Sigmoid (hard $_{\sigma}$)	$\max\left(0, \min\left(1, \frac{(x+1)}{2}\right)\right)$
Soft-Sign Sigmoid (SoftSign)	$x/(1+ x)$
Snake Periodic Function (Snake)	$x + \sin^2(ax)/a$
Linearly Scaled Hyperbolic Tangent (LiSHT)	$x \cdot \tanh(x)$
Rectified Linear Unit (ReLU)	$\max(0, x)$
Exponential Linear Unit (ELU)	$\max(0, x) + \min(0, \alpha(e^x - 1))$
Gaussian Error Linear Unit (GELU)	$x\mathcal{P}(X \leq x), X \sim \mathcal{N}(0, 1)$
Scaled Exponential Linear Unit (SELU)	$\gamma(\max(0, x) + \min(0, \alpha(e^x - 1)))$
Sigmoid-Weighted Linear Units (Swish β)	$\frac{x}{1+e^{-\beta x}}$
Self Regularized Non-Monotonic Neural (Mish)	$x \tanh(\log(1 + e^x))$

TABLE III: Gated Linear Unit (GLU) functions with different activations

Models	Activation functions	GLU form functions
BilinearGLU	Linear	$(xW + b) \odot (xV + c)$
GLU	Sigmoid	$\sigma(xW + b) \odot (xV + c)$
hardGLU	hard $_{\sigma}$	$\text{hard}_{\sigma}(xW + b) \odot (xV + c)$
SoftsignGLU	SoftSign	$\text{Softsign}(xW + b) \odot (xV + c)$
SnakeGLU	Snake	$\text{Snake}(xW + b) \odot (xV + c)$
LiGLU	LiSHT	$\text{LiSHT}(xW + b) \odot (xV + c)$
ReGLU	ReLU	$\max(0, xW + b) \odot (xV + c)$
EGLU	ELU	$\text{ELU}(xW + b) \odot (xV + c)$
GEGLU	GELU	$\text{GELU}(xW + b) \odot (xV + c)$
SeGLU	SELU	$\text{SELU}(xW + b) \odot (xV + c)$
SwiGLU	Swish β	$\text{Swish}\beta(xW + b) \odot (xV + c)$
MiGLU	Mish	$\text{Mish}(xW + b) \odot (xV + c)$

TABLE IV: Gated Non-Linear Unit (GnLU) functions with different activations

Models	Activation functions	GnLU functions
GnLU	Sigmoid	$\sigma(xW + b) \odot \sigma(xV + c)$
LiGnLU	LiSHT	$\text{LiSHT}(xW + b) \odot \text{LiSHT}(xV + c)$
MiGnLU	Mish	$\text{Mish}(xW + b) \odot \text{Mish}(xV + c)$
SeGnLU	SELU	$\text{SELU}(xW + b) \odot \text{SELU}(xV + c)$
SwiGnLU	Swish β	$\text{Swish}\beta(xW + b) \odot \text{Swish}\beta(xV + c)$

supervised classification. The results demonstrate significant improvements in flexibility and performance in these areas.

Initialize the parameters of the neural network. In a loop, draw minibatch samples from the joint distribution of X and Z, and additional samples from the marginal distribution of Z. Compute the lower bound of the mutual information estimate using the neural network's output. Then, calculate the gradient of this estimate, adjusting for bias. Update the network parameters with this gradient and repeat until the process converges.

D. Integrating GRN to Attention Mechanism

Fig. 2 provided demonstrates the progression of the attention mechanism in a Transformer architecture, starting with the original multi-head attention and evolving to incorporate GRN. Initially, the standard multi-head attention mechanism linearly transforms inputs to create queries, keys, and values, applying

softmax to their dot products for attention weighting, followed by concatenation and a dense layer to generate outputs. The evolved mechanism introduces a GRN between the softmax and concatenation steps, allowing the model to capture more complex temporal dependencies within the data. Finally, the complete Transformer model with multi-head GRN-Attention is shown, retaining the original structure but replacing the standard attention with the GRN-variant. This modification suggests a focus on enhancing the model's sequential processing capabilities, potentially improving its performance on tasks requiring a nuanced understanding of time-dependent patterns in data.

IV. EXPERIMENTAL RESULTS

To effectively assess the performance of our method, metrics including accuracy, precision, recall (or sensitivity), and F1

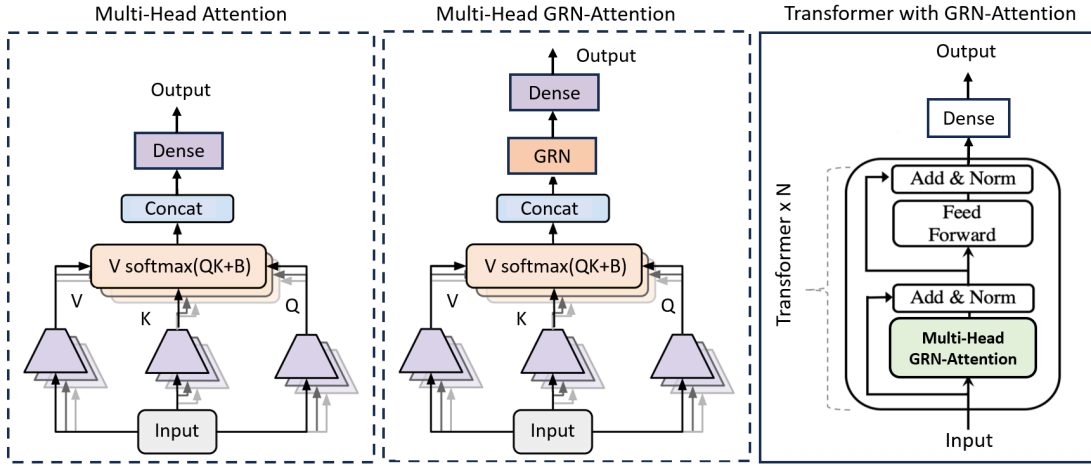


Fig. 2: An end-end process diagram workflow demonstration.

TABLE V: Hyperparameters of classifiers

Hyperparameters	Transformer
Hidden layers	4
Number of neurons	128
Number of multi-heads attention	4
Batch size	96
Dropout	0.25
Learning rate	6e-04
Optimizer	Adam

Algorithm 1 Mutual Information Neural Estimation (MINE)

- 1: $\theta \leftarrow$ Initialize network parameters
- 2: **repeat**
- 3: Sample a minibatch of b pairs $(x^{(i)}, z^{(i)})$ from the joint distribution \mathbb{P}_{XZ}
- 4: Independently sample b instances $\tilde{z}^{(i)}$ from the marginal distribution \mathbb{P}_Z
- 5: Compute the empirical lower bound $V(\theta)$:

$$V(\theta) \leftarrow \frac{1}{b} \sum_{i=1}^b T_{\theta}(x^{(i)}, z^{(i)}) - \log \left(\frac{1}{b} \sum_{i=1}^b e^{T_{\theta}(x^{(i)}, \tilde{z}^{(i)})} \right)$$

- 6: Calculate bias-corrected gradient estimates:

$$G(\theta) \leftarrow \nabla_{\theta} V(\theta)$$
- 7: Update the network parameters using gradient ascent:

$$\theta \leftarrow \theta + \alpha G(\theta)$$

- 8: **until** convergence is reached

score. These metrics are defined as follows:

$$\text{Accuracy (acc)} = \frac{\text{TP} + \text{TN}}{\text{TP} + \text{TN} + \text{FP} + \text{FN}}$$

$$\text{Precision (pre)} = \frac{\text{TP}}{\text{TP} + \text{FP}}$$

$$\text{Recall/Sensitivity (rec)} = \frac{\text{TP}}{\text{TP} + \text{FN}}$$

$$\text{F1-Score (f1)} = \frac{2 * \text{Precision} * \text{Recall}}{\text{Precision} + \text{Recall}}$$

where TN and TP stand for true negative and true positive, respectively, and they are the number of negative and positive patients that are classified correctly. Whereas FP and FN represent false positive and false negative, respectively, and they represent the number of positive and negative patients that were wrongly predicted.

TABLE VI: GLU Models' Performance

Models	Acc	Pre	Rec	F1
BilinearGLU	0.97	0.90	0.94	0.92
GLU	0.98	0.90	0.97	0.93
hardGLU	0.97	0.89	0.93	0.91
SoftSignGLU	0.97	0.91	0.93	0.92
SnakeGLU	0.97	0.91	0.92	0.92
LiGLU	0.97	0.91	0.94	0.92
ReGLU	0.97	0.89	0.94	0.92
EGLU	0.97	0.93	0.92	0.92
GEGLU	0.97	0.88	0.94	0.91
SeGLU	0.97	0.90	0.93	0.92
SwiGLU	0.97	0.91	0.93	0.92
MiGLU	0.98	0.91	0.95	0.93

The Table VI provides a comprehensive comparison of various Gated Linear Unit (GLU) model variants across four key performance metrics: Accuracy (Acc), Precision (Pre), Recall (Rec), and F1 Score (F1). Among these, the GLU and MiGLU models emerge as the top performers. Both models achieve the highest accuracy, with a score of 0.98, indicating their superior overall prediction correctness. The

Algorithm 2 Mutual Information Neural Estimation (MINE) for a GRN-Transformer

Require: Encoded representations **before_grn** and **after_grn**, Target labels **y**

- 1: **procedure** MINE
- 2: **function** INITIALIZEMINEMODEL(input_shape)
- 3: Define a neural network with input shape *input_shape* and output of size 2
- 4: **return** Initialized neural network
- 5: **end function**
- 6: **function** COMPUTEMI(data, y, model)
- 7: **shuffled_y** \leftarrow **shuffle**(y)
- 8: **joint_pred** \leftarrow **model**([data, y])
- 9: **marginal_pred** \leftarrow **model**([data, shuffled_y])
- 10: $MI \leftarrow E[\mathbf{joint_pred}] - \log(E[\exp(\mathbf{marginal_pred})])$
- 11: **return** *MI*
- 12: **end function**
- 13: *model_before_grn* \leftarrow INITIALIZEMINEMODEL(shape_of(**before_grn**[1]))
- 14: *model_after_grn* \leftarrow INITIALIZEMINEMODEL(shape_of(**after_grn**[1]))
- 15: **for** *epoch* = 1 to *num_epochs* **do**
- 16: Train *model_before_grn* on **before_grn** and **y**
- 17: Train *model_after_grn* on **after_grn** and **y**
- 18: **end for**
- 19: *MI_before* \leftarrow COMPUTEMI(*before_grn*, *y*, *model_before_grn*)
- 20: *MI_after* \leftarrow COMPUTEMI(*after_grn*, *y*, *model_after_grn*)
- 21: **Print**("MI before GRN: ", *MI_before*)
- 22: **Print**("MI after GRN: ", *MI_after*)
- 23: **end procedure**

MiGLU model leads in precision, boasting a score of 0.91, which suggests it is particularly effective in making accurate positive predictions with the least false positives. On the other hand, the GLU model excels in recall with a top score of 0.97, highlighting its capability in correctly identifying the majority of true positive cases. Furthermore, both these models share the highest F1 score of 0.93, illustrating their optimal balance between precision and recall. The GLU and MiGLU models demonstrate the best overall performance among the variants, making them potentially more effective for tasks requiring high accuracy, precise predictions, and reliable identification of true positives.

TABLE VII: GnLU Models' Performance

Models	Acc	Pre	Rec	F1
GnLU	0.98	0.91	0.96	0.94
LiGnLU	0.97	0.91	0.92	0.91
MiGnLU	0.97	0.90	0.94	0.92
SeGnLU	0.97	0.91	0.93	0.92
SwiGnLU	0.97	0.90	0.92	0.91

The Table VII provides a detailed comparison of various Gated Non-linear Unit (GnLU) model variants, evaluated on key performance metrics: Accuracy (Acc), Precision (Pre), Recall (Rec), and F1 Score (F1). Among these, the standard GnLU model distinctly outperforms its counterparts. It achieves the highest accuracy at 0.98, indicating superior overall prediction correctness, and leads in precision with a score of 0.91, highlighting its effectiveness in making accurate positive predictions with minimal false positives. Additionally,

the GnLU model excels in recall with the highest score of 0.96, demonstrating its capability in correctly identifying the vast majority of true positive cases. Furthermore, it achieves the top F1 score of 0.94, indicating an optimal balance between precision and recall. This comprehensive performance makes the GnLU model highly effective and reliable in diverse scenarios, particularly in tasks where high precision and accurate identification of true positives are crucial.

The provided Fig. 5 depict the performance of a GRN-Transformer with a Gated Non-Linear Unit (GNLU) across various training epochs, showing metrics for both training and validation data. The loss graph shows a typical sharp decline in loss for both training and validation at the start of training, which stabilizes as epochs increase, indicating that the model is learning and generalizing well without signs of overfitting. The AUC graph reveals high and stable values for both sets, suggesting excellent class separation capability. Precision and recall both start low but rise quickly to plateau at high values, which demonstrates that the model accurately identifies true positives and covers a high proportion of actual positive samples. The close proximity of training and validation curves across all metrics indicates that the model is generalizing well to new data. There's some fluctuation in validation loss, but it's within normal bounds, suggesting some variability in the validation set or learning process. Overall, these results point to a well-performing model with strong classification abilities, pending further evaluation in the context of specific project goals and benchmarks.

The Fig. 7 displays the performance of a Transformer model with GRN-Attention over 140 epochs, showing key metrics

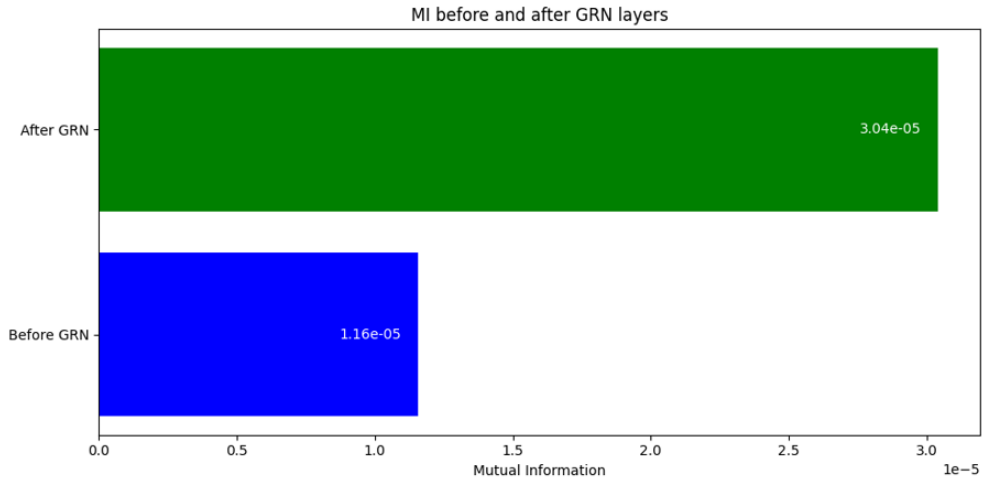


Fig. 3: An end-end process diagram workflow demonstration.

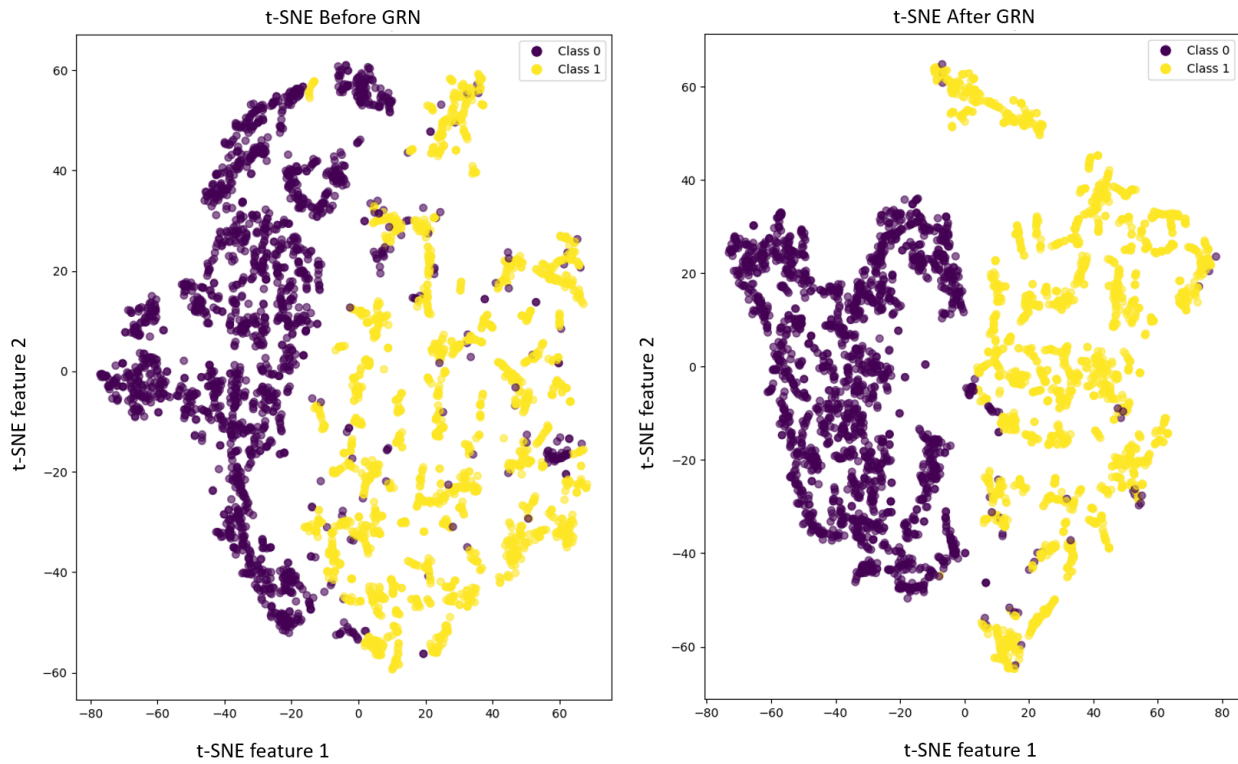


Fig. 4: An end-end process diagram workflow demonstration.

for training and validation datasets. The loss graph indicates an initial decrease in both training and validation losses, with subsequent fluctuations in validation loss hinting at potential overfitting. The AUC scores begin high and plateau, but a widening gap between training and validation suggests the model may be learning training-specific patterns that don't generalize well. Precision and recall metrics are initially volatile but stabilize, though they exhibit considerable noise, especially in the validation set. This noise implies inconsistency in the model's predictive accuracy and sensitivity to positive samples. While the model shows initial solid learning, the observed metrics suggest it may be overfitting to the training data. Measures such as regularization, hyperparameter tuning,

or early stopping may be necessary to improve the model's generalization to new data and ensure stable performance across all metrics.

V. CONCLUSION

This study embarks on an exploration of the Transformer model's performance in various learning environments, with a focus on the Gated Residual Network Transformer (GRN-Transformer). Initial findings reveal that Transformers trained via supervised learning are outperformed by other neural networks such as MLP, CNN, and LSTM. Subsequently, it is observed that employing unsupervised and self-supervised

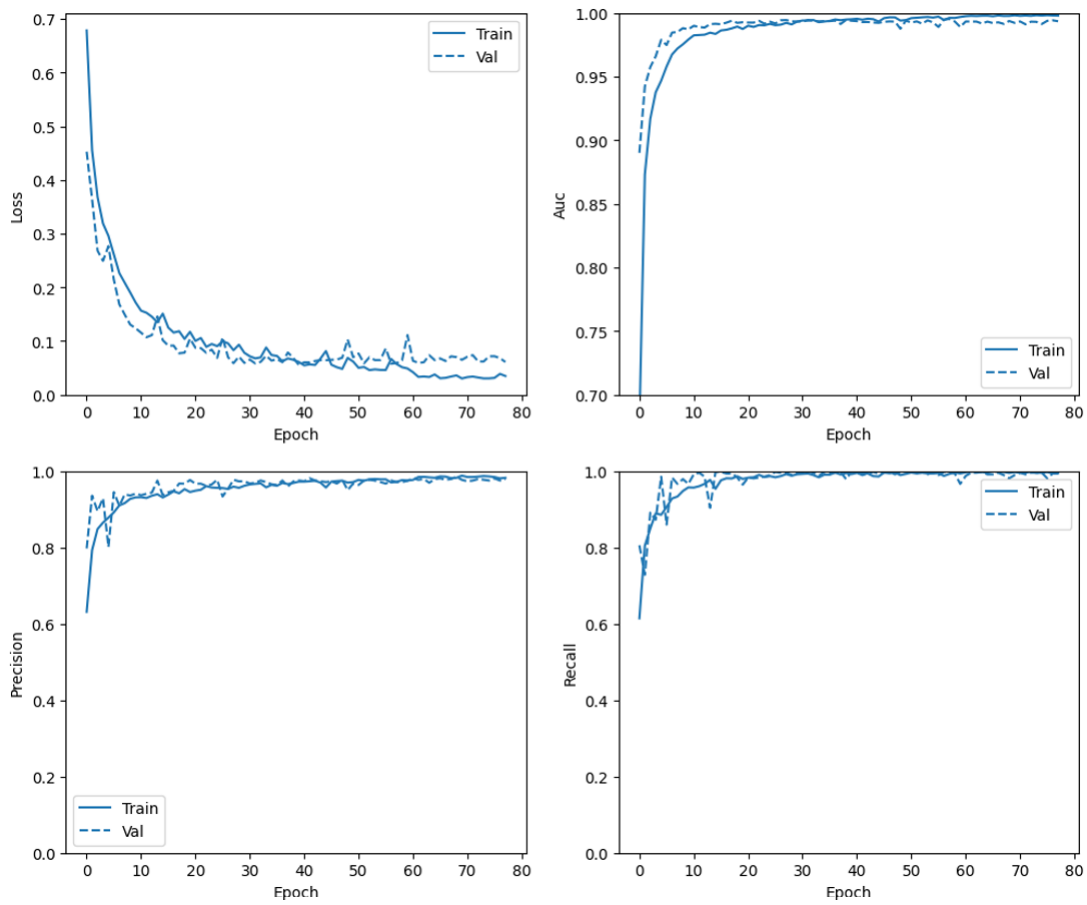


Fig. 5: Learning curve during training and validation for the GRN-Transformer with Gated Non-Linear Unit.

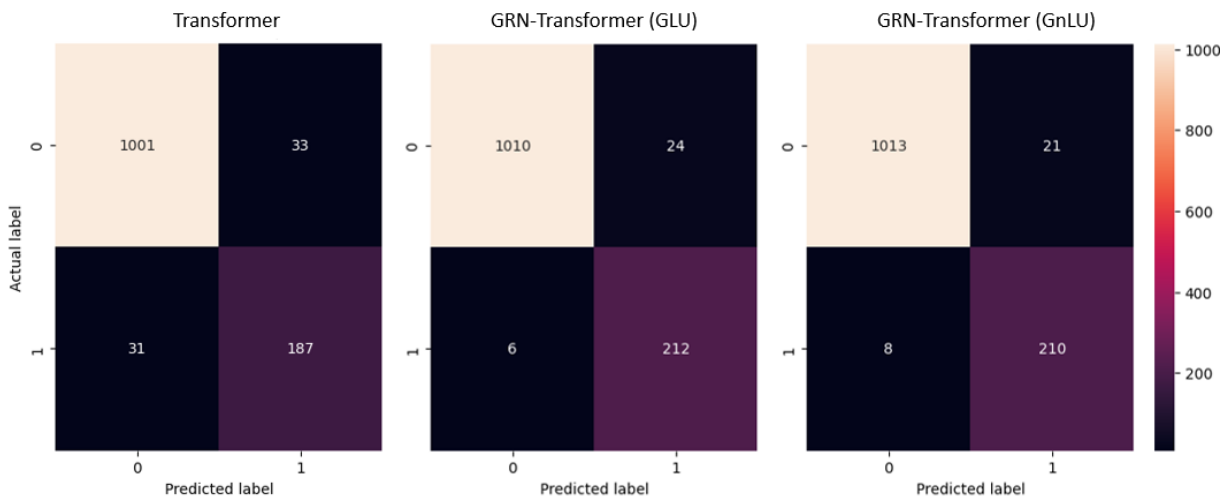


Fig. 6: An end-end process diagram workflow demonstration.

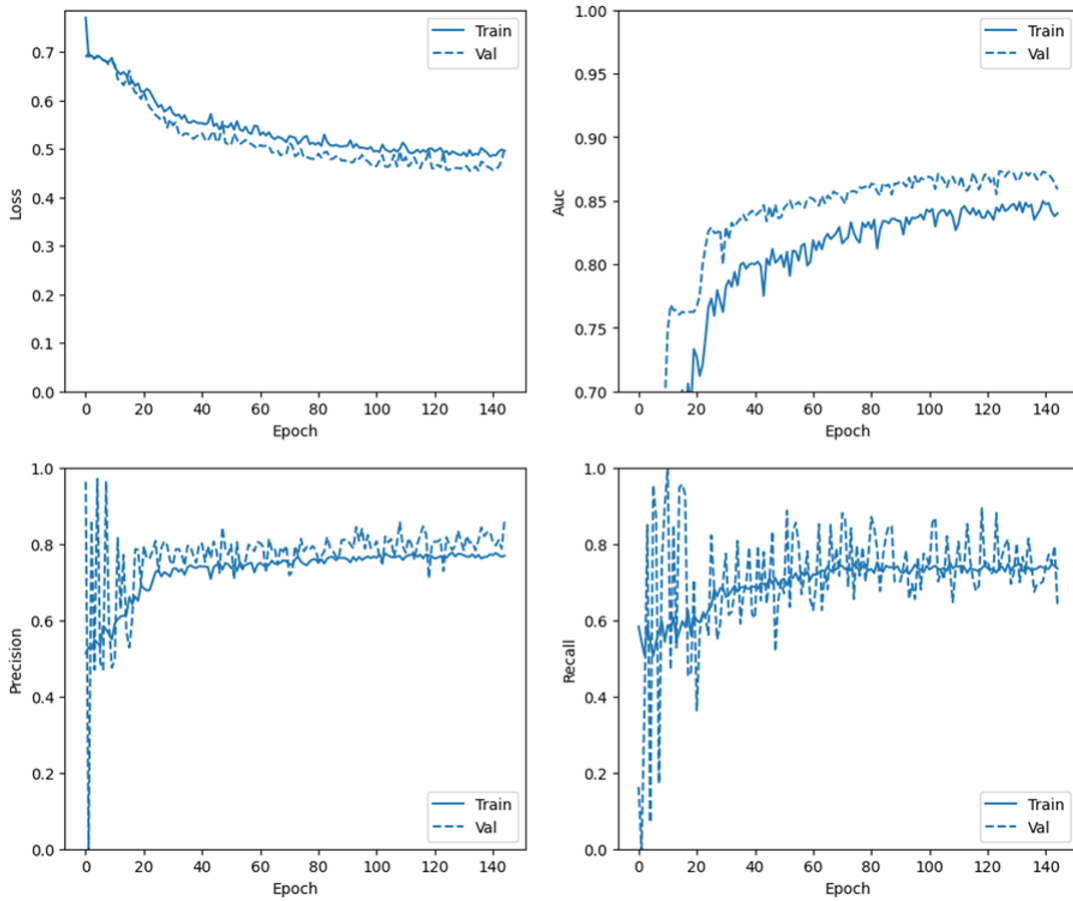


Fig. 7: An end-end process diagram workflow demonstration.

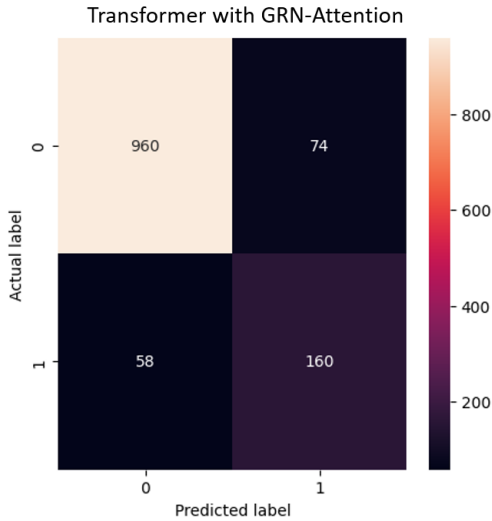


Fig. 8: An end-end process diagram workflow demonstration.

learning techniques on unannotated data, followed by fine-tuning on annotated data, substantially enhances the performance of the Transformer model. Despite these improvements, these methods still fall short of the performance level achieved by the GRN-Transformer.

Aiming to delve deeper into this phenomenon, our research

pivots to analyze different activation functions for the Gated Linear Unit (GLU), a crucial component of the GRN structure. The study employs Mutual Information Neural Estimation (MINE) to verify the effectiveness of GRN. Additionally, it investigates the positional impact of GRN within the Transformer architecture, particularly examining its role as an intermediate layer within the Attention mechanism as opposed to an external intermediary layer.

The experimental results of this study are threefold. Firstly, they confirm that Gated Non-linear Units (GnLU) utilizing sigmoid activation outperform other variants across all evaluated metrics. Secondly, the application of MINE corroborates that GRN enhances the mutual information between hidden representations and output. Thirdly, positioning GRN as an intermediate layer, acting as a filter to eliminate irrelevant information and amplify relevant data, proves to be more effective than integrating it within the Attention mechanism.

In conclusion, this study sheds light on the mechanisms through which GRN enhances the performance of GRN-Transformers, surpassing other learning methods such as unsupervised or self-supervised learning. These insights are particularly valuable in fields like PPG artifact detection in PICU environments, where data availability is limited, providing a pathway for the adoption of advanced models like Transformers in such challenging contexts.

ACKNOWLEDGMENT

The Research Center at CHU Sainte-Justine Hospital, University of Montreal, provided the clinical PPG data. The authors thank Clara Macabiau and Dr. Kevin Albert for their support in data preprocessing and annotating for this research.

REFERENCES

- [1] D. Brossier, R. El Taani, M. Sauthier, N. Roumeliotis, G. Emeriaud, and P. Jouvét, "Creating a high-frequency electronic database in the picu: the perpetual patient," *Pediatr. Crit. Care Med.*, vol. 19, no. 4, pp. e189–e198, 2018.
- [2] N. Roumeliotis, G. Parisien, S. Charette, E. Arpin, F. Brunet, and P. Jouvét, "Reorganizing care with the implementation of electronic medical records: a time-motion study in the picu," *Pediatr. Crit. Care Med.*, vol. 19, no. 4, pp. e172–e179, 2018.
- [3] A. Mathieu and et. al., "Validation process of a high-resolution database in a pediatric intensive care unit—describing the perpetual patient's validation," *Journal of Evaluation in Clinical Practice*, vol. 27, no. 2, pp. 316–324, 2021.
- [4] A. C. Dziorny and et. al., "Clinical decision support in the picu: Implications for design and evaluation," *Pediatr. Crit. Care Med.*, vol. 23, no. 8, pp. e392–e396, 2022.
- [5] T.-D. Le and et. al., "Detecting of a patient's condition from clinical narratives using natural language representation," *IEEE Open J. Eng. Med. Biol.*, vol. 3, pp. 142–149, 2022.
- [6] M. Sauthier, G. Tuli, P. A. Jouvét, J. S. Brownstein, and A. G. Randolph, "Estimated pao₂: A continuous and noninvasive method to estimate pao₂ and oxygenation index," *Critical care explorations*, vol. 3, no. 10, 2021.
- [7] G. Emeriaud, Y. M. López-Fernández, N. P. Iyer, M. M. Bembea, A. Agulnik, R. P. Barbaro, F. Baudin, A. Bhalla, W. B. De Carvalho, C. L. Carroll, et al., "Executive summary of the second international guidelines for the diagnosis and management of pediatric acute respiratory distress syndrome (palicc-2)," *Pediatr. Crit. Care Med.*, vol. 24, no. 2, p. 143, 2023.
- [8] P. Jouvét and et. al., "A pilot prospective study on closed loop controlled ventilation and oxygenation in ventilated children during the weaning phase," *Critical Care*, vol. 16, no. 3, pp. 1–9, 2012.
- [9] M. Wysocki, P. Jouvét, and S. Jaber, "Closed loop mechanical ventilation," *J. Clin. Monit. Comput.*, vol. 28, pp. 49–56, 2014.
- [10] B. L. Hill and et. al., "Imputation of the continuous arterial line blood pressure waveform from non-invasive measurements using deep learning," *Scientific reports*, vol. 11, no. 1, p. 15755, 2021.
- [11] F. Fan and et. al., "Estimating spo₂ via time-efficient high-resolution harmonics analysis and maximum likelihood tracking," *IEEE J. Biomed. Health Inform.*, vol. 22, no. 4, pp. 1075–1086, 2017.
- [12] C. Macabiau, T.-D. Le, K. Albert, P. Jouvét, and R. Noumeir, "Label propagation techniques for artifact detection in imbalanced classes using photoplethysmogram signals," *arXiv preprint arXiv:2308.08480*, 2023.
- [13] T.-D. Le, C. Macabiau, K. Albert, P. Jouvét, and R. Noumeir, "Grn-transformer: Enhancing motion artifact detection in picu photoplethysmogram signals," *arXiv preprint arXiv:2308.03722*, 2023.
- [14] T.-D. Le, "Boosting transformer's robustness and efficacy in PPG signal artifact detection with self-supervised learning," *arXiv preprint arXiv:2401.01013*, 2024.
- [15] M. I. Belghazi, A. Baratin, S. Rajeshwar, S. Ozair, Y. Bengio, A. Courville, and D. Hjelm, "Mutual information neural estimation," in *International conference on machine learning*. PMLR, 2018, pp. 531–540.
- [16] T.-D. Le and et. al., "A small-scale switch transformer and nlp-based model for clinical narratives classification," *arXiv preprint arXiv:2303.12892*, 2023.
- [17] M. Clara and et. al., "Label propagation techniques for artifact detection in imbalanced classes using photoplethysmograph signals," *Submitted to IEEE for possible publication*, 2023.
- [18] S. H. Lee and et. al., "Vision transformer for small-size datasets," *arXiv preprint arXiv:2112.13492*, 2021.
- [19] R. Shao and X.-J. Bi, "Transformers meet small datasets," *IEEE Access*, vol. 10, pp. 118 454–118 464, 2022.
- [20] M. Hahn, "Theoretical limitations of self-attention in neural sequence models," *Trans. Assoc. Comput. Linguist.*, vol. 8, pp. 156–171, 2020.
- [21] T. Sattler and et. al., "Understanding the limitations of cnn-based absolute camera pose regression," in *IEEE/CVF conference on computer vision and pattern recognition*, 2019, pp. 3302–3312.
- [22] Y. N. Dauphin and et. al., "Language modeling with gated convolutional networks," in *International Conference on ML*, 2017, pp. 933–941.
- [23] M. Liu and et. al., "Gated transformer networks for multivariate time series classification," *arXiv preprint arXiv:2103.14438*, 2021.
- [24] B. Lim, S. Ö. Arık, N. Loeff, and T. Pfister, "Temporal fusion transformers for interpretable multi-horizon time series forecasting," *International Journal of Forecasting*, vol. 37, no. 4, pp. 1748–1764, 2021.
- [25] P. Savarese and D. Figueiredo, "Residual gates: A simple mechanism for improved network optimization," in *Int. Conf. Learn. Represent.*, 2017.
- [26] A. D. Rasamoelina, F. Adjailia, and P. Sinčák, "A review of activation function for artificial neural network," in *2020 IEEE 18th World Symposium on Applied Machine Intelligence and Informatics (SAMII)*. IEEE, 2020, pp. 281–286.
- [27] J. Lederer, "Activation functions in artificial neural networks: A systematic overview," *arXiv preprint arXiv:2101.09957*, 2021.



Thanh-Dung Le (Member, IEEE) received a B.Eng. degree in mechatronics engineering from Can Tho University, Vietnam, an M.Eng. degree in electrical engineering from Jeju National University, S. Korea, and a Ph.D. in biomedical engineering from École de Technologie Supérieure (ETS), Canada. He is a postdoctoral fellow at the Biomedical Information Processing Laboratory, ETS. His research interests include applied machine learning approaches for biomedical informatics problems. Before that, he joined the Institut National de la Recherche Scientifique, Canada, where he researched classification theory and machine learning with healthcare applications. He received the merit doctoral scholarship from Le Fonds de Recherche du Québec Nature et Technologies. He also received the NSERC-PERSWADE fellowship, Canada, and a graduate scholarship from the Korean National Research Foundation, S. Korea.



Philippe Jouvét received the M.D. degree from Paris V University, Paris, France, in 1989, the M.D. specialty in pediatrics and the M.D. subspecialty in intensive care from Paris V University, in 1989 and 1990, respectively, and the Ph.D. degree in pathophysiology of human nutrition and metabolism from Paris VII University, Paris, in 2001. He joined the Pediatric Intensive Care Unit of Sainte Justine Hospital—University of Montreal, Montreal, QC, Canada, in 2004. He is currently the Deputy Director of the Research Center and the Scientific Director of the Health Technology Assessment Unit, Sainte Justine Hospital—University of Montreal. He has a salary award for research from the Quebec Public Research Agency (FRQS). He currently conducts a research program on computerized decision support systems for health providers. His research program is supported by several grants from the Sainte-Justine Hospital, Quebec Ministry of Health, the FRQS, the Canadian Institutes of Health Research (CIHR), and the Natural Sciences and Engineering Research Council (NSERC). He has published more than 160 articles in peer-reviewed journals. Dr. Jouvét gave more than 120 lectures in national and international congresses.



Rita Noumeir (Member, IEEE) received master's and Ph.D. degrees in biomedical engineering from École Polytechnique of Montreal. She is currently a Full Professor with the Department of Electrical Engineering, École de Technologie Supérieure (ETS), Montreal. Her main research interest is in applying artificial intelligence methods to create decision support systems. She has extensively worked in healthcare information technology and image processing. She has also provided consulting services in large-scale software architecture, healthcare interoperability, workflow analysis, and technology assessment for several international software and medical companies, including Canada Health Infoway.